Published by Avanti Publishers

Global Journal of Energy Technology Research Updates

ISSN (online): 2409-5818

Optimization of Solar Photovoltaics Tilt Angle for Hybrid Solar-Geothermal Heat Pump Applications in Extreme Cold Climate Regions of Northwestern Ontario, Canada

Basel I. Ismail* and Anjali Nagi

Department of Mechanical & Mechatronics Engineering, Lakehead University, 955 Oliver Road, Thunder Bay, Ontario P7B5E1, Canada

ARTICLE INFO

Article Type: Research Article

Academic Editor: Haifan Liang

Keywords:
Solar photovoltaic systems
Cold climate energy systems
Renewable energy optimization
Geothermal heat pump systems
Sustainable energy technologies
Hybrid renewable energy systems

Timeline:
Received: October 01, 2025
Accepted: November 15, 2025
Published: December 05, 2025

Citation: Ismail BI, Nagi A. Optimization of solar photovoltaics tilt angle for hybrid solar-geothermal heat pump applications in extreme cold climate regions of Northwestern Ontario, Canada. Glob J Energ Technol Res Updat. 2025; 12: 1-16.

DOI: https://doi.org/10.15377/2409-5818.2025.12.1

ABSTRACT

The global imperative to mitigate greenhouse gas emissions, combat air pollution, and manage escalating energy costs and demand underscores the critical role of renewable energy technologies. Solar photovoltaic (PV) systems present a viable solution by directly converting sunlight into electricity, especially for energy-intensive facilities in regions with high solar potential, such as Northwestern Ontario, Canada. The tilt angle of a PV panel is a fundamental parameter that significantly influences the amount of incident solar radiation, thereby directly affecting the system's power output and overall economic efficiency. This study employs location-specific experimental data and validated numerical modeling to determine the optimal monthly and annual tilt angles for a PV array intended to potentially power a geothermal heat pump (GHP) at the Thunder Bay Regional Health Sciences Centre located in a severe cold climate region of Northwestern Ontario. Optimizing this angle enhances efficiency, reduces operating costs, and improves the commercial viability of the hybrid system. Analysis revealed that the monthly optimal tilt angle varies from 3° in June to a maximum of 69° in December and January. The annual fixed-angle optimum is approximately 39°. Solar irradiance peaks in June at roughly 5.14 kWh/m², falling to its annual minimum in December at about 49.2% of this peak. To specifically support the GHP during its peak heating demand, a winter-optimized tilt of 67° is recommended. This configuration captures an average maximum of 3.14 kWh/m²/day during the coldest months, aligning solar energy harvest with the facility's highest heating loads. Furthermore, the site experiences a substantial variation in available solar energy hours, with monthly average daily daylight hours ranging from a low of 8.2 hours (in December) to a high of 15.8 hours (in June). The estimated annual optimum tilt angle of 39° for TBRHSC aligns with the 31°–45° range reported for similar latitudes, and the corresponding predicted solar irradiance of 3.94 kWh/m²/day shows good agreement (<7% difference) with international benchmarks. The study's primary applied contribution is the proposal of a load-specific, winter-optimized tilt of 67°—a strategic adaptation designed to enhance the technical and economic feasibility of integrated solar-GHP systems operating under the harsh climatic constraints of Northwestern Ontario.

*Corresponding Author
Email: bismail@lakeheadu.ca
Tel: +(1) 807-766-7100

©2024 Ismail and Nagi. Published by Avanti Publishers. This is an open access article licensed under the terms of the Creative Commons Attribution Non-Commercial License which permits unrestricted, non-commercial use, distribution and reproduction in any medium, provided the work is properly cited. (http://creativecommons.org/licenses/by-nc/4.0/)

1. Introduction

Solar photovoltaic systems are known for their capabilities and have been used in many applications to directly convert the renewable solar energy into electrical energy for locations with abundant solar energy where there is a desperate need and demand for electrical power. Thunder Bay city ($48^o\ 24'\text{N}, 89^o\ 14'\ \text{W}$) is located on the Northwestern shore of Lake Superior. As the largest city in Northwestern Ontario, it serves as a regional hub for commerce, education, healthcare, and transportation. With a population of approximately 108,000 as of the latest census [1]. The climate in the Thunder Bay area is typical of a mid-latitude inland location with a lake moderating influence. The city experiences a large variation in weather throughout the year. More particularly, it experiences a humid continental climate, characterized by long, cold winters and short, warm summers, with average annual temperatures ranging from -13°C in January to 18°C in July [2]. Thunder Bay has an abundant solar radiation. It has a yearly average daily bright sunshine hours of 2130 [2] and annual average daily solar insolation of 3.41 kWh/m^2 [3]. Thunder Bay's unique combination of natural resources, climate challenges, and community-driven initiatives makes it an ideal case study for exploring renewable energy applications. Its efforts to integrate green energy solutions into municipal and commercial infrastructure offer valuable insights into how smaller cities can lead the way in combating climate change while addressing local energy needs.

Located in the heart of Thunder Bay, the Thunder Bay Regional Health Sciences Centre (TBRHSC) serves as the primary healthcare facility for Northwestern Ontario, offering advanced medical care to a population spread across a vast geographical area. TBRHSC plays a vital role in fostering healthcare innovation and education in the region. The facility is renowned for its commitment to providing comprehensive and specialized care, including cancer treatment, cardiac services, and emergency medicine. With its expansive infrastructure and 375 inpatient beds, the hospital operates year-round with substantial energy demands, making it a critical focal point for energy efficiency and sustainability initiatives [4]. Currently, the hospital aims to reduce its natural gas consumption by 5% over five years (2025-2029) and by 8% by 2035, while also targeting a 3% reduction in overall energy consumption per square foot within the next five years and a 6% reduction by 2035. These measures align with the facility’s commitment to reducing greenhouse gas (GHG) emissions by 10% from 2016 levels by 2035, in accordance with Ontario's broader goal of a 30% reduction from 2005 levels by 2030. Furthermore, TBRHSC's strategic initiatives demonstrate a commitment to integrating energy management into daily operations, prioritizing indoor environmental quality, operational efficiency, and sustainability in decision-making processes. This forward-thinking approach creates a conducive environment for exploring geothermal energy solutions, which could significantly contribute to achieving the hospital's energy conservation and GHG reduction targets. The adoption of a renewable geothermal heating and cooling system would align with TBRHSC's goals of reducing reliance on fossil fuels, enhancing operational efficiency, and promoting sustainability, while also addressing the hospital's unique energy demands. This will play a crucial role in identifying the potential benefits and challenges associated with integrating geothermal energy into TBRHSC’s infrastructure [4]. A photograph showing an aerial view of TBRHSC is shown in Fig. (**1a**) [4], and the map location of the health facility is shown in Fig. (**1b**) [5]. To reduce its dependence on fossil fuels and lower operational costs, a solar-powered geothermal heat pump (GHP) system is a potential attractive solution. The integration of solar photovoltaics (PV) with geothermal heat pumps (GHPs) presents a highly efficient and sustainable approach to a building’s heating and cooling system. A GHP system requires electricity to operate key components such as the compressor, circulating pumps, and fans, which facilitate heat exchange between the ground and the building. By using solar PV arrays to generate this electricity, the system can significantly reduce reliance on the grid and fossil fuels, lowering operational costs and carbon emissions, making it a viable solution for facilities like TBRHSC. The tilt angle of a PV panel relative to the horizontal plane is a critical parameter directly impacting the system's power output and overall efficiency. This angle determines the amount of incident solar radiation received by the PV surface. The tilt angle of a photovoltaic (PV) panel is a critical determinant of system performance, directly governing electrical output and overall efficiency [6]. For a fixed-tilt array, optimizing this angle for a specific geographical location is therefore essential to maximize annual energy yield. At at the Thunder Bay Regional Health Sciences Centre (TBRHSC) site, such optimization is paramount; positioning the PV array at its ideal tilt not only captures more solar energy but also reduces the required array area for a given electrical load. This reduction in physical footprint lowers capital expenditure and significantly enhances the economic viability of the proposed hybrid solar PV-GHP system—a principle that applies equally to thermal solar collectors.

Figure (1a): An arial view of Thunder Bay Regional Health Sciences Centre, Thunder Bay, Northwestern Ontario [4], a potential application of the hybrid Solar PV-GHP system.

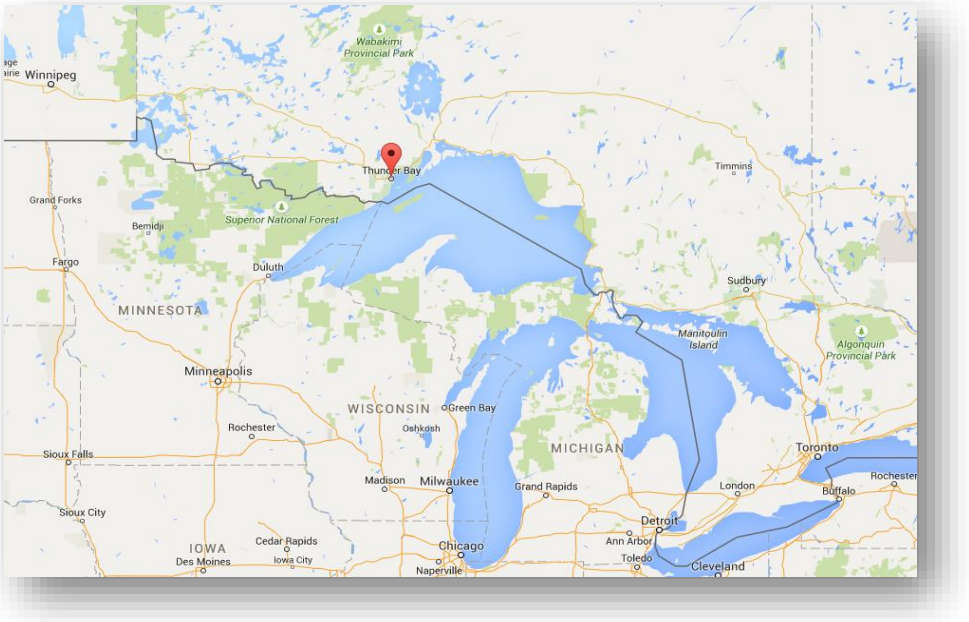

Figure (1b): Map Location of TBRHSC, Thunder Bay (48.38 ^{0}N, 89.25 ^{0}W), Ontario, Canada [5].

While extensive experimental and numerical studies have investigated PV tilt angle and orientation with applications [7-38], this work employs a location-specific experimental data (via measurements) with well-established and validated mathematical model, originally developed by Liu and Jordan (1962) [39] and extended by Klein (1977) [40]. The model was used to estimate the total solar radiation incident on an inclined surface and to determine the specific optimum tilt angle for maximizing generation from a PV array for powering a GHP potential application system at TBRHSC. Through detailed numerical simulations and analysis, the total solar energy on an optimally inclined surface was computed for all months and aggregated seasonally. Furthermore, the yearly averaged optimum tilt angle for the site was determined. This analysis provides actionable insights for

increasing the overall efficiency and operational cost savings of the proposed hybrid solar PV-GHP system at TBRHSC. By maximizing energy harvest through precise tilt angle configuration, this work directly improves the commercial feasibility of large-scale implementation at TBRHSC, where the economic advantages become most pronounced. Therefore, maximizing the capture of incident solar energy at TBRHSC through precise tilt optimization is paramount.

2. Mathematical Model and Computation Methodology

Leveraging the widely validated mathematical framework established in [8-13, 17-37], the monthly average daily solar radiation, $\bar{H}_T$, incident upon an unshaded sloped PV panel, is estimated. This calculation assumes a PV panel tilted at an angle β relative to the horizontal plane, situated at a latitude ϕ north of the Equator, and oriented directly toward the Equator such that the solar azimuth angle, $\gamma = 0$. The governing equation is expressed as follows:

$$\bar{H}_T = \bar{H}_{b,T} + \bar{H}_{d,T} + \bar{H}_{g,T} \tag{1}$$

Equation (1) defines the total solar radiation, $\bar{H}_T$ (kWh/m²), as the aggregate of three distinct irradiance vectors interacting with the inclined surface. This composite value is modeled as the summation of: (1) the beam (direct) radiation, $\bar{H}_{b,T}$; (2) the sky-diffuse radiation, $\bar{H}_{d,T}$; and (3) the ground-reflected radiation, $\bar{H}_{g,T}$. The mathematical expressions governing each of these constituent components are presented as follows:

$$\bar{H}_{b,T} = \bar{H}\left(1 - \frac{\bar{H}_d}{\bar{H}}\right)\bar{R}_b \tag{2}$$

$$\bar{H}_{d,T} = \bar{H}_d\left(\frac{1+\cos\beta}{2}\right) \tag{3}$$

$$\bar{H}_{g,T} = \bar{H}\,\bar{\rho}_g\left(\frac{1-\cos\beta}{2}\right) \tag{4}$$

A fundamental premise of this calculation is the assumption that both the sky-diffuse and ground-reflected radiation components incident on the tilted surface are isotropic—meaning the radiation flux is uniformly distributed from all directions. Consequently, this modeling approach is precisely termed the isotropic sky model. Fig. (**2**) visually details the key solar angles utilized in the geometric calculations of this model [41]. In the above equations, the term $\bar{H}$ (kWh/m^2) and is the monthly average daily total terrestrial radiation incident on a horizontal surface (i.e. $\beta = 0$); $\bar{H}_d$ (/kWhm^2) is the monthly average daily sky-diffuse radiation incident on a horizontal surface; and $\bar{\rho}_g$ is the monthly average daily ground reflectivity (also known as albedo). The ratio $\frac{\bar{H}_d}{\bar{H}}$ is computed using the following correlations [6,13,14]:

(a) For $\omega_s \le 81.4^o$ and $0.3 \le \bar{K}_T \le 0.8$, the following equation is implemented:

$$\left(\frac{\bar{H}_d}{\bar{H}}\right) = 1.391 - 3.560\,\bar{K}_T + 4.189\,\left(\bar{K}_T\right)^2 - 2.137\,\left(\bar{K}_T\right)^3 \tag{5}$$

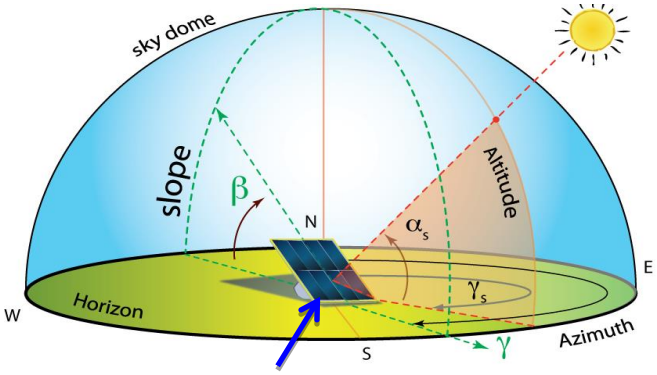

Figure 2: A conceptual illustration showing basic solar angles used in this study [41

(b) For $\omega_s > 81.4^o$ and $0.3 \le \bar{K}_T \le 0.8$, the following relationship, however, is applied:

$$\left(\frac{\bar{H}_d}{\bar{H}}\right) = 1.311 - 3.022\ \bar{K}_T + 3.427\ \left(\bar{K}_T\right)^2 - 1.821\ \left(\bar{K}_T\right)^3 \tag{6}$$

In both equations above, the sunset hour angle ω_s can be determined using:

$$\omega_s = cos^{-1}(-\tan\varphi\ \tan\delta) \tag{7}$$

where, the solar declination angle δ as a function of the day in the year *n* is calculated using:

$$\delta = 23.45\ sin\left[360\ \frac{(284+n)}{365}\right] \tag{8}$$

The monthly average daily clearness index $\bar{K}_T$ given in Equations (5) and (6) above is given by:

$$\bar{K}_T = \frac{\bar{H}}{\bar{H}_o} \tag{9}$$

where, $\bar{H}_o$ is monthly average daily extraterrestrial radiation received on a horizontal surface, estimated by:

$$\bar{H}_o = \frac{24*3600*1367}{\pi}\left(1+0.033\cos\frac{360*n}{365}\right)*\left(\cos\varphi\cos\delta\sin\omega_s + \frac{\pi\omega_s}{180}\sin\varphi\sin\delta\right) \tag{10}$$

In Equation (10), $\bar{H}_0$ is in J/m^2 (divide by 3.6x10^6 to convert it to kWh/m^2). In this work, location-specific $\bar{H}$ data for the TBRHSC location were experimentally measured using a HOBO micro-solar-weather station, as shown in Fig. (**3**). A solar radiation sensor specifically a HOBO silicon pyranometer smart sensor was used to measure the average light intensity with a light sensor. This type of pyranometer can measure solar irradiance up to 1280 W/m^2, at a temperature of -40°C. The pyranometer has an operating range of 0 W/m^2 to 1280 W/m^2 with a spectral range of 300 to 1100 nm, and least count of 0.1 W/m^2. Solar global radiation data, $\bar{H}$, measured using the pyranometer of the solar-logging station were used to numerically estimate the monthly optimum tilt angles for the solar PV panel. The $\bar{H}$ measured values and the estimated $\bar{H}_o$ (using Equation 10) are compared and shown in Fig. (**4**).

Figure 3: Photograph and schematic diagram showing the solar-logging station used for measuring the monthly average daily solar radiation received on a horizontal surface positioned on Lakehead University's campus nearby TBRHSC site for use as inputs into the mathematical predictive model.

In Equation (2), the parameter $\overline{R}_b$ is known as the beam geometric factor for the mean day of the month, expressed by:

$$\overline{R}_b = \frac{\cos(\varphi-\beta)\cos\delta\sin\omega_s^{'} + (\pi/180)\ \omega_s^{'}\sin(\varphi-\beta)\sin\delta}{\cos\varphi\cos\delta\sin\omega_s + (\pi/180)\ \omega_s\sin\varphi\sin\delta} \tag{11}$$

where, $\omega_s^{'}$ is the sunset hour angle for the tilted surface for the mean day of the month, which is given by:

$$\omega_s^{'} = \min\begin{bmatrix} \cos^{-1}(-\tan\varphi\tan\delta) \\ \cos^{-1}(-\tan(\varphi-\beta)\tan\delta) \end{bmatrix} \tag{12}$$

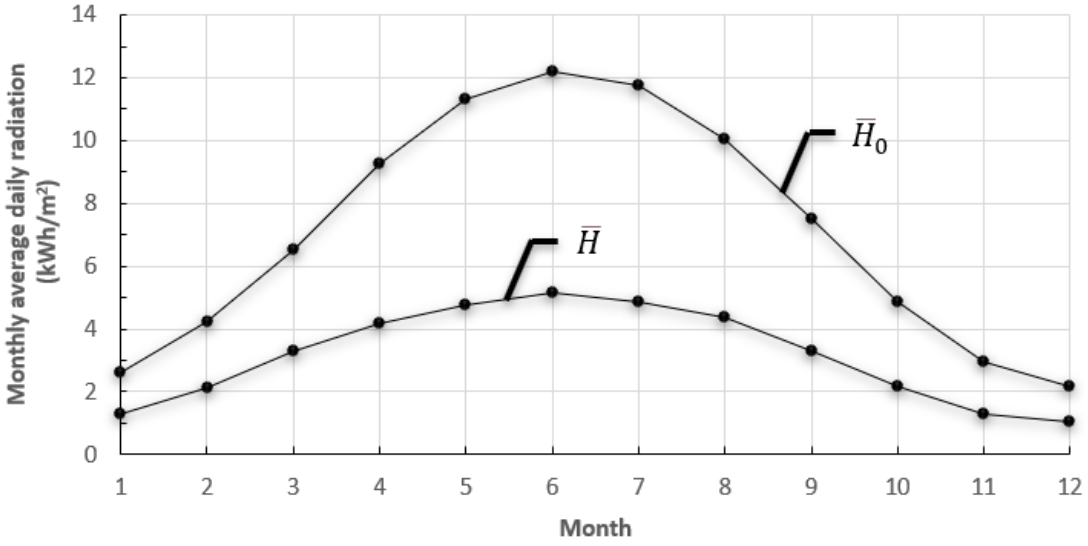

Figure 4: Comparison of the monthly average daily solar radiation (extraterrestrial vs. terrestrial) incident on a horizontal PV panel at TBRHSC site.

where, "min" means the smaller of the two terms in the brackets. The monthly average daily number of sunlight hours can be computed using:

$$N = \frac{2}{15}\cos^{-1}\left(-\tan\varphi\tan\delta\right) \tag{13}$$

The yearly average monthly optimum tilt angle for the PV system installed at TBRHSC site can be determined using the simple mathematical relationship given by:

$$\left(\bar{\beta}_{opt}\right)_{year} = \frac{\sum_{Jan}^{Dec}\beta_{opt}}{12} \tag{14}$$

A schematic diagram showing a flowchart summarizing the computation process is shown in Fig. (**5**). The computational procedure for this study was implemented systematically by utilizing the complete set of Equations (1) through (12). For every month of the year, computations were performed using the mean day to represent the month's average conditions. The key methodology involved iteratively varying the inclination (tilt) angle, β, 0^0 (horizontal) to 90^o (vertical) in increments of 3^o. For each increment and month, the total solar radiation, $\bar{H}_T$, was computed. The resulting values of $\bar{H}_T$ were then rigorously compared to identify the angle that produced the maximum solar energy reception, thus, called $\bar{H}_{T,\max}$. This maximizing angle was subsequently assigned as the optimum monthly mean daily tilt angle ($\bar{\beta}_{opt}$). This detailed simulation and iterative comparison process was repeated across all twelve months, as depicted in the methodological flowchart (Fig. **5**), to determine the full sequence of optimum monthly tilt angles for the solar PV panel installation proposed for the TBRHSC site.

3. Results and Discussion

Following the application of the mathematical model and the location-specific data along with the computational procedure detailed in the preceding section, the subsequent findings are presented and analyzed here. A primary focus of this analysis is the monthly variation in atmospheric transmittance, governed by a parameter known as the the monthly average daily clearness index, $\bar{k}_T$. Fig. (**6**) provides a comparative visualization of the monthly average daily clearness index, $\bar{k}_T$, across the entire year. Analysis of these computed values reveals that the maximum clearness index, occurring in March, reached a peak value of approximately 55%.

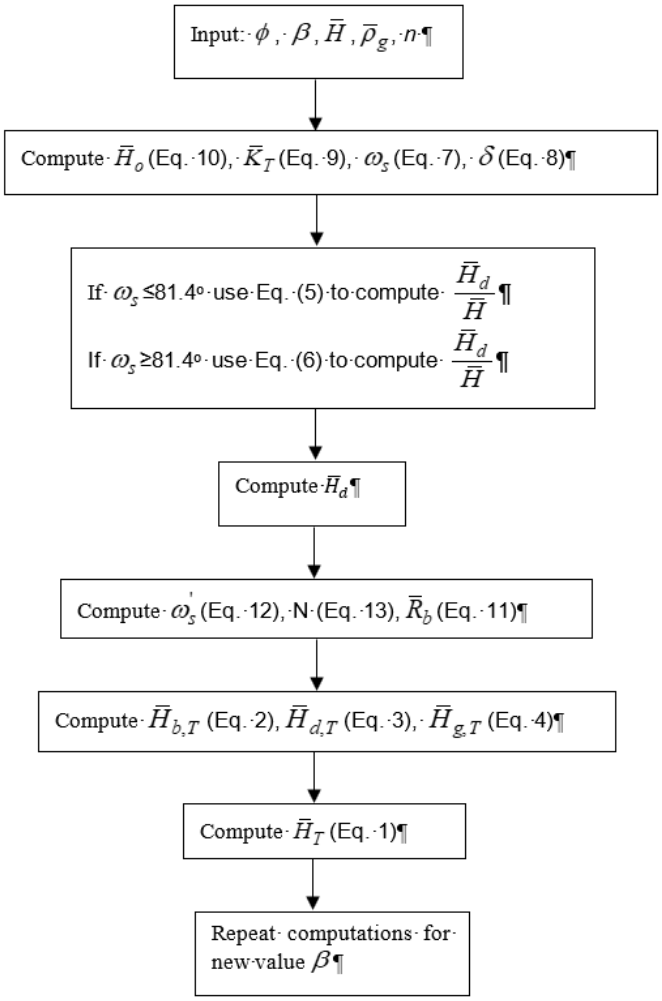

Figure 5: A schematic showing a flowchart for performing numerical simulations used in this study.

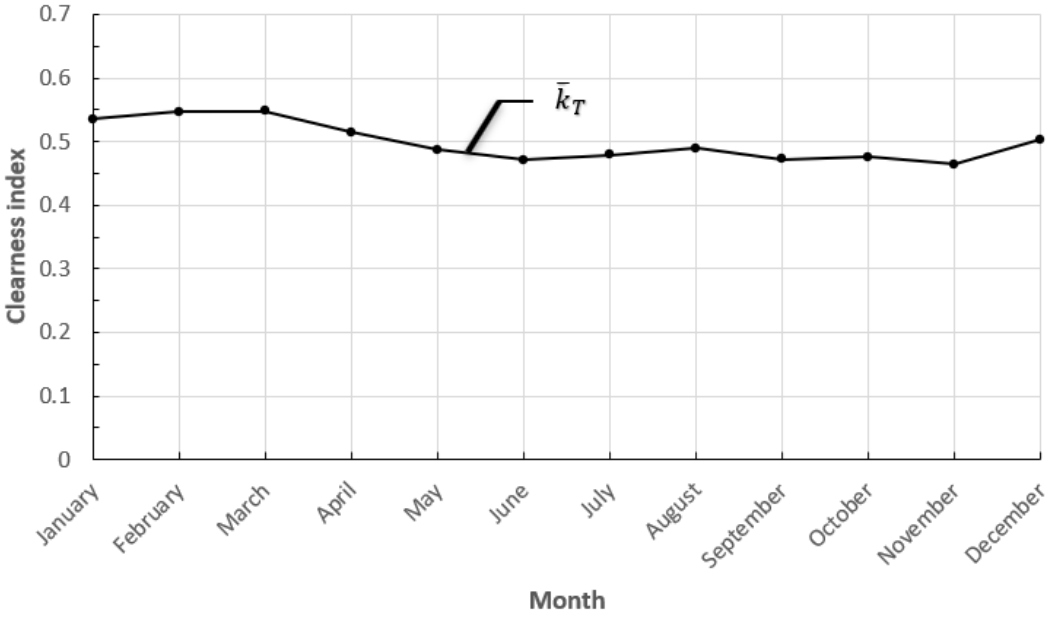

Figure 6: The estimated monthly average daily clearness index for a solar PV panel at TBRHSC site.

Conversely, the minimum observed value, approximately 46%, was recorded in the month of November. Fig. (**7**) presents a comparative analysis of the ratio of sky-diffuse radiation $\bar{H}_d$ to the total global radiation $\bar{H}$ incident on a horizontal surface across all months of the year. This ratio exhibited variation between approximately 0.347 and 0.457. The maximum value occurred in June (45.7%), while the minimum was recorded in February (34.7%). This outcome specifically indicates that the monthly average daily sky-diffuse component of radiation received on a horizontal surface at the proposed TBRHSC site reached its highest relative contribution in June, accounting for nearly 46% of the total incident global radiation.

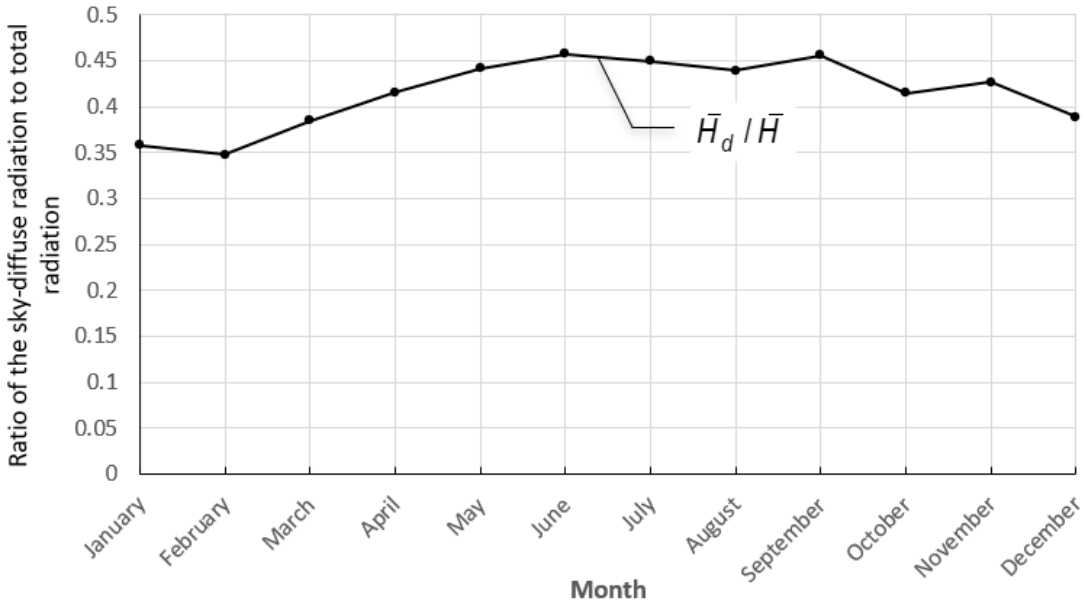

Figure 7: The estimated ratio of the monthly average daily diffuse solar radiation to global radiation incident on a horizontal PV panel at TBRHSC site.

Fig. (**8**) presents a comparative analysis of the estimated monthly average daily total solar radiation, $\bar{H}_T$, incident upon a tilted PV panel at the TBRHSC site for the cold winter season, represented by the months of December, January, and February. Across nearly all tilt angles, the month of February consistently exhibited the

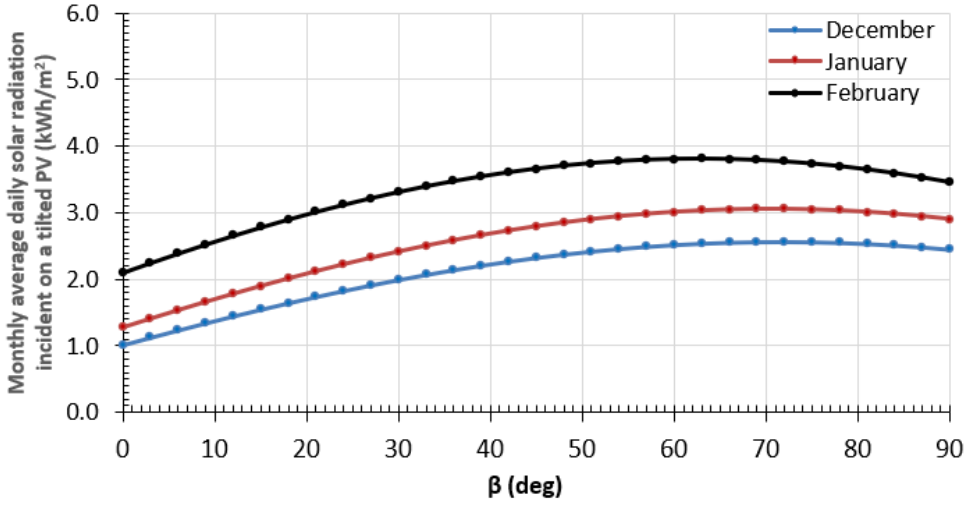

Figure 8: Comparison of the estimated monthly average daily solar radiation incident on a tilted PV panel at TBRHSC site, for the cold season (months of December, January and February) as a function of the PV module tilt angle.

highest estimated $\bar{H}_T$ values compared to December and January. Specifically, the maximum incident solar radiation in February reached approximately 3.81 kWh/m^2 at a tilt angle of 63^o. In contrast, the maximum incident solar radiation for December was 2.56 kWh/m^2 and January was 3.05 kWh/m^2, both occurred at a steeper tilt angle of approximately 69^o. It should be noted that a steeper tilt angle in the winter season also enhances self-cleaning of snow upon falling on the PV panels. The numerical simulations result also show that the minimum incident solar radiation for all three months occurred when the PV panel was positioned horizontally (β = 0^0). A key observation is the monotonically rapid increase in incident solar radiation for all three months as the tilt angle increased from the horizontal, stabilizing significantly after the tilt angle reached approximately 60^o. Based on this analysis, the estimated average optimum tilt angle for the PV panel potential installation at the TBRHSC site during the winter season was approximately 66^o, resulting in an average maximum incident solar radiation of 3.14 kWh/m^2.

Fig. (**9**) presents a comparison of the estimated monthly average daily solar radiation, $\bar{H}_T$, incident upon a tilted PV panel at the TBRHSC site for the spring season (March, April, and May) as a function of the tilt angle. A notable observation is the significantly decreasing optimum tilt angle required to achieve maximum incident solar radiation across these three months. For March, the maximum incident solar radiation of approximately 4.39 kWh/m^2 occurred at an optimum tilt angle ($\bar{\beta}_{opt}$) of 51^o. Conversely, as the sun's altitude increases toward summer, the optimum angles shifted to much smaller values for April ($\bar{\beta}_{opt}$ =30^o) and May ($\bar{\beta}_{opt}$ =12^o), yielding higher corresponding maximum incident radiation values of 4.57 kWh/m^2 and 4.79 kWh/m^2, respectively. For the month of May, the dependency of $\bar{H}_T$ on the tilt angle demonstrates a particularly sharp peak: the incident solar radiation initially increased slowly as the tilt angle moved from 0^o to the optimum 12^o, but then decreased rapidly as the panel angle continued to increase, hitting a minimum value of approximately 2.21 kWh/m^2 when the panel was positioned vertically (β = 90^0). For the spring season at TBRHSC site, the highest minimum value of the monthly average incident solar radiation of approximately 2.21 kWh/m2 on the vertically positioned PV panel occurred in the month May. The average optimum tilt angle of the PV panel at TBRHSC site for the spring season was approximately 31o. Fig. (10) shows a comparison of the estimated monthly average daily incident solar radiation at TBRHSC site for the summer season (months of June, July and August) as a function of tilt angle of the PV

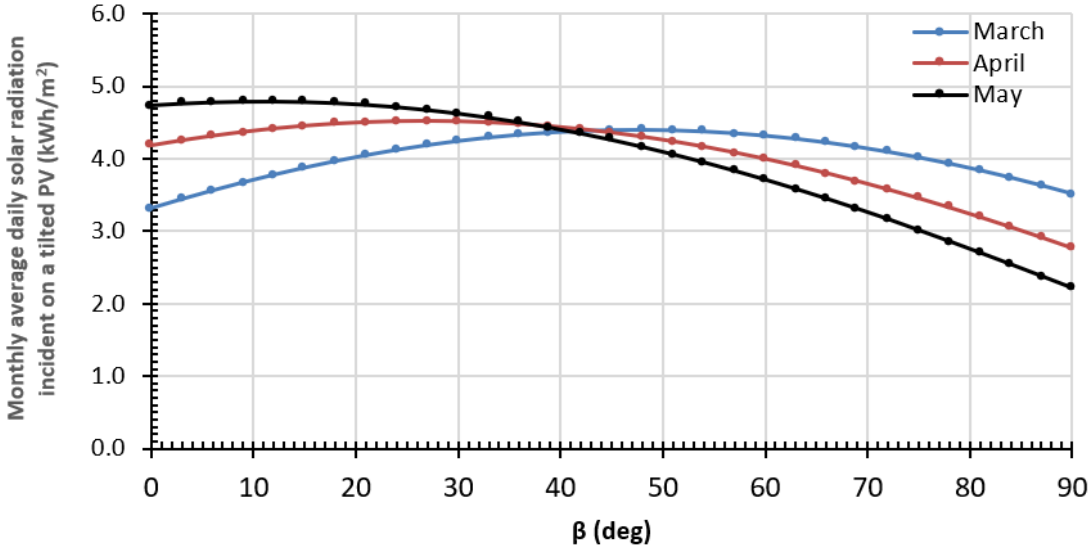

Figure 9: Comparison of the estimated monthly average daily solar radiation incident on a tilted PV panel at TBRHSC site, for the spring season (months of March, April, and May) as a function of the PV panel tilt angle.

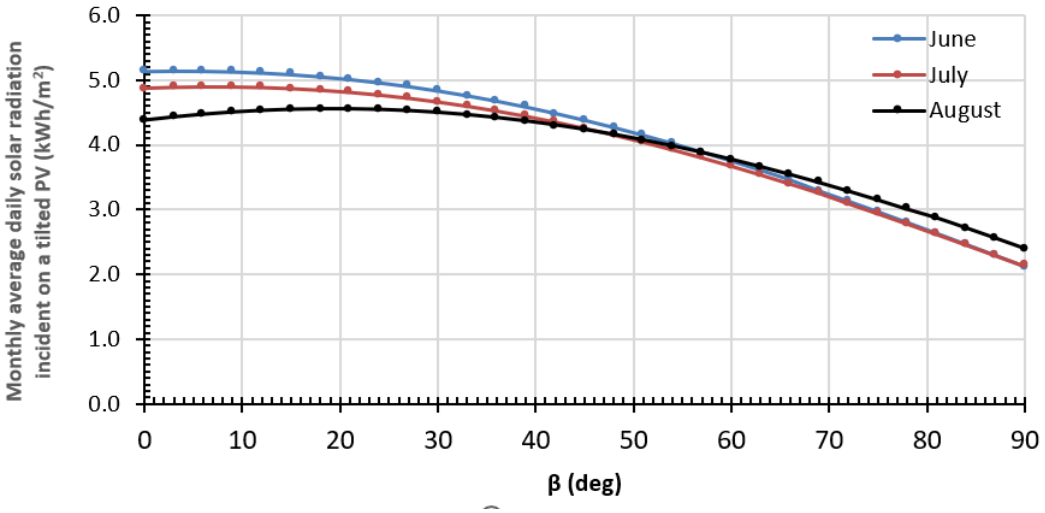

Figure 10: Comparison of the estimated monthly average daily solar radiation incident on a tilted PV panel at TBRHSC site, for the summer season (months of June, July, and August) as a function of the PV panel tilt angle.

Panel. The incident solar radiation profiles for June and July exhibit a high degree of similarity, while both significantly differ from the August profile. The optimum tilt angle ($\bar{\beta}_{opt}$) was minimal during the peak summer months: June recorded the lowest ($\bar{\beta}_{opt}$) at 3°, yielding the maximum incident solar radiation of nearly 5.14 kWh/m^2. This value dropped slightly to 4.90 kWh/m^2 in July at an optimum tilt of 9°. A distinct shift occurred in August, where the required optimum tilt angle rose considerably to 21°, and the maximum incident solar radiation decreased to approximately 4.55 kWh/m^2 relative to the preceding months. Based on these simulation results, the average optimum inclination angle for the PV panel at the TBRHSC site during the entire summer season was computed to be approximately 11°, corresponding to an average maximum incident solar radiation of nearly 4.86 kWh/m^2.

The estimated monthly average daily solar radiation, $\bar{H}_T$, incident on the inclined PV panel at the TBRHSC site for the months of September, October, and November (representing the autumn/fall season), as a function of the panel's tilt angle, is visually compared in Fig. (**11**). The dependence of incident solar radiation on the PV panel's tilt angle exhibits a pronounced variation across the three autumn months. The analysis reveals a sequential increase in the required optimum tilt angle as the sun's position lowers toward the winter solstice: the $\bar{\beta}_{opt}$ values for

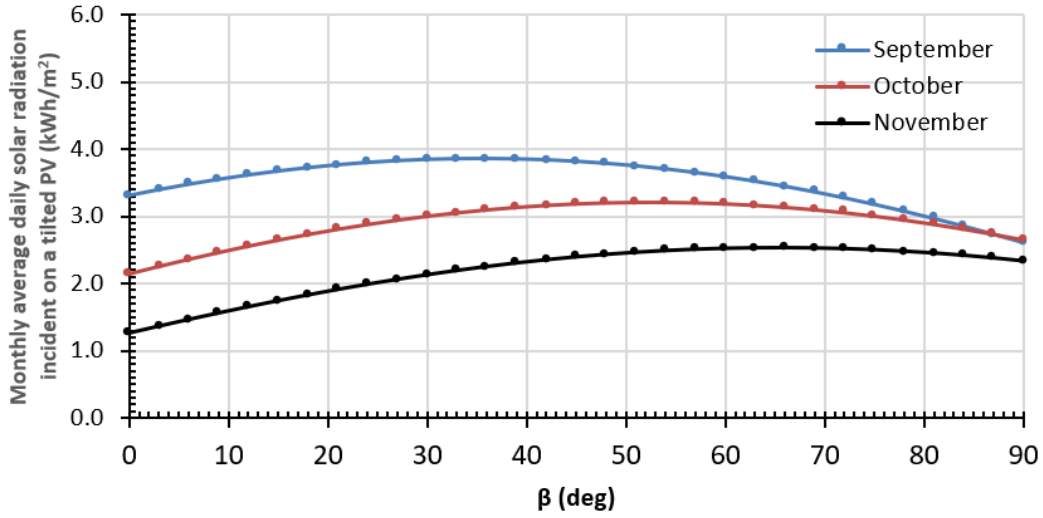

Figure 11: Comparison of the estimated monthly average daily solar radiation incident on a tilted PV panel at TBRHSC site, for the Fall season (months of September, October, and November) as a function of the PV module tilt angle.

September, October, and November are 33°, 51°, and 66°, respectively. These optimum orientations yield corresponding estimated maximum incident solar radiation values of 3.86 kWh/m^2, 3.22 kWh/m^2, and 2.53 kWh/m^2, respectively. Consistent with the shifting solar path, the highest incident radiation in the autumn season occurred in September (3.86 kWh/m^2 at $\bar{\beta}_{opt}$ = 33°). A notable trend across all three months is the rapid, substantial increase in incident solar radiation observed at relatively low tilt angles, indicating high sensitivity to initial orientation adjustments. For the purpose of fixed-angle deployment, the computed average optimum tilt angle for the entire autumn season is approximately 50°, resulting in an average maximum incident radiation of approximately 3.20 kWh/m^2.

Fig. (**12**) provides a comprehensive comparison of the estimated maximum monthly average daily solar radiation incident on an optimally tilted PV module at the TBRHSC site throughout the year. A comprehensive comparison across the entire year reveals that the highest maximum monthly average daily incident radiation $\bar{H}_{T,\max}$ occurred in June 5.14 kWh/m^2. This peak production sharply contrasts with the lowest annual value, recorded in November, which reached only approximately 49.2% of the June maximum. It is critically important to note the correlation between the maximum solar resource and the PV array orientation: the June peak was achieved with a near-horizontal optimum tilt angle of only 3^0.

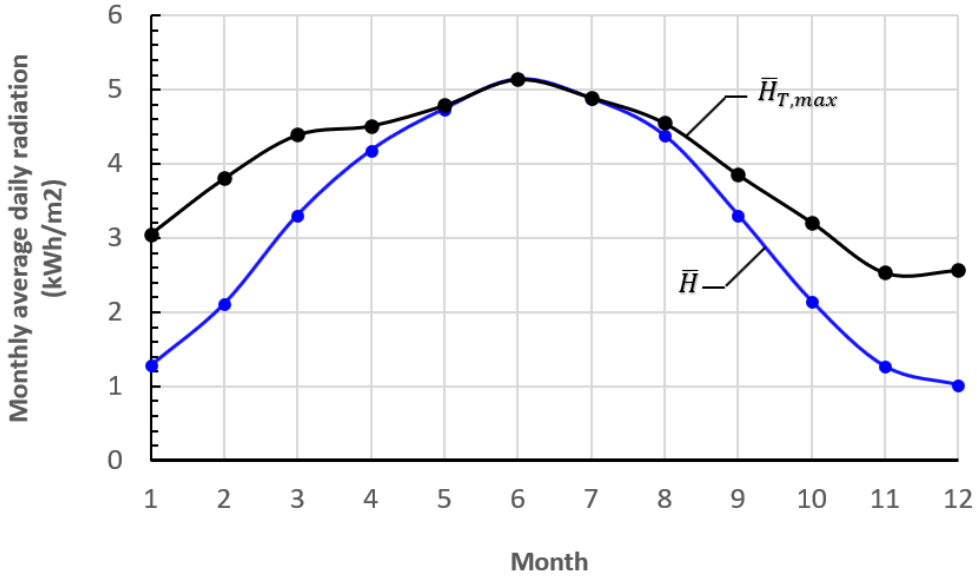

Figure 12: Comparison of the estimated maximum monthly average daily solar radiation incident on an optimally tilted PV panel at TBRHSC site as a function of the month in the year.

The comprehensive results, including the monthly optimum tilt angles, their respective maximum incident radiation values, and the corresponding monthly average daylight hours, are summarized in Table **1**. Based on the computed monthly variations, the final estimated yearly average monthly optimum tilt angle for the PV system potential installation at the TBRHSC site is 39°. Furthermore, the site experiences a substantial variation in available solar energy hours, with monthly average daily daylight hours ranging from a low of 8.2 hours (in December) to a high of 15.8 hours (in June), as shown in Table **1**.

Table **2** shows a comparison of the annual average optimum tilt angle ($\bar{\beta}_{opt}$) determined in the present study for Thunder Bay Regional Health Sciences Centre (TBRHSC), Thunder Bay, Canada, with corresponding values reported in reference [11] for global sites of comparable latitude. All angles are measured from the horizontal plane and are optimized for maximal annual energy yield of fixed-tilt photovoltaic (PV) systems. Data from [11] are included to contextualize the locally derived result within established international findings. The annual optimum tilt angle determined in this study, $\bar{\beta}_{opt}$ =39°, aligns well with the established literature for comparable latitudes. As presented in Table **2**, a comparison with the comprehensive global analysis by [11] for analogous geographical

locations shows that the value of 39° falls within the reported global range of annual optimum tilt angles, which spans from 30° to 45°. Further quantitative validation is provided by comparing the resultant solar energy yield.

Table 1: Summary of monthly optimum tilt angles and their corresponding maximum incident monthly average daily solar radiation and daylight hours for the tilted solar PV panel at TBRHSC site.

Month	β_{opt} (Degrees)	$\bar{H}_{T,\max}$ (kWh/m^2)	N (Hours)
Jan	**69**	**3.05**	**8.6**
Feb	**63**	**3.81**	**10.0**
Mar	**48**	**4.40**	**11.6**
Apr	**27**	**4.52**	**13.4**
May	**12**	**4.79**	**15.0**
Jun	**3**	**5.14**	**15.8**
Jul	**9**	**4.90**	**15.5**
Aug	**21**	**4.55**	**14.1**
Sep	**33**	**3.86**	**12.3**
Oct	**51**	**3.22**	**10.5**
Nov	**66**	**2.53**	**9.0**
Dec	**69**	**2.56**	**8.2**
	$\left(\bar{\beta}_{opt}\right)_{year}$ **= 39°**		

Table 2: Comparative analysis of annual optimum tilt angles for mid-latitude, Northern Hemisphere of cold climates locations [11].

Location	ϕ (Degrees)	β_{opt} (Degrees)
Calgary, Canada	**51.12**	**45**
Vancouver, Canada	**49.18**	**34**
Thunder Bay, Canada (this study)	**48.38**	**39**
London, UK	**51.15**	**34**
St. Hubert, Belgium	**50.03**	**35**
Ostrava, Czech Rep.	**49.72**	**33**
Cologne, Germany	**50.87**	**32**
Munich, Germany	**48.13**	**33**
Hungary, Debrecen	**47.48**	**30**
Luxembourg, Luxembourg	**50.03**	**35**
Bielsko-Biala, Poland	**49.67**	**31**
Kosice, Slovakia	**48.70**	**33**
Beek, Netherlands	**50.92**	**34**
Ulaanbaatar, Mongolia	**47.93**	**43**

For the comparable-latitude locations cited in [11], the annual average maximum daily solar radiation incident on optimally tilted photovoltaic (PV) panels is approximately 4.23 kWh/m². The corresponding simulation for the present study yields a value of 3.94 kWh/m². This represents a relative difference of approximately 6.9%, which is within an acceptable margin of error for comparative solar energy studies considering variations in local atmospheric conditions, measurement methodologies, and specific albedo. The close agreement in both the optimal tilt angle parameter and the consequent energy irradiation estimates demonstrates that the findings of this study are consistent with broader international data, thereby reinforcing the methodological validity and regional applicability of the results.

This study's approach aligns with the well-established theoretical foundation of optimizing tilt angle to maximize solar yield, a common focus in PV literature. Its novelty lies in the specific application: tailoring this optimization not for general annual yield, but to meet the distinct seasonal load profile of a proposed geothermal heat pump at a critical facility TBRHSC. While the radiation modeling is standard, the integration of load-matching—proposing a winter-optimized tilt angle (67°) to align with peak heating demand—represents a context-driven advancement beyond typical single-parameter optimization. The validation of the annual optimum tilt (39°) against international benchmarks confirms methodological rigor, while the load-specific recommendation demonstrates the study's applied contribution to improving the viability of integrated renewable energy systems in extreme cold climate of Northwestern Ontario, Canada.

4. Conclusions

Solar photovoltaic (PV) technology is emerging as a predominant source of new electricity generation capacity in Canada, driven by climate policy imperatives such as greenhouse gas (GHG) mitigation, alongside structural shifts in the energy sector. This rapid adoption underscores the technology's growing strategic importance within the national energy portfolio. The Thunder Bay Regional Health Sciences Centre (TBRHSC) presents a compelling use-case for solar PV deployment. Its geographical context—characterized by a relatively remote location, rising community energy demand, and significant solar resource availability—makes on-site generation both a practical and strategic asset. To maximize the return on such an investment, system efficiency is paramount. Among the critical design parameters, the PV panel's tilt angle relative to the horizontal plane exerts a profound influence on incident solar irradiance and, consequently, electrical energy yield. This study employed an established mathematical model to compute the total solar radiation incident on an inclined surface, with the objective of determining the optimum tilt angles for a proposed PV system powering a geothermal heat pump (GHP) application at TBRHSC. Optimizing this parameter is essential for enhancing overall system efficiency, reducing operating costs, and improving the commercial viability of a fully PV-powered GHP system. Key findings indicate that the monthly average optimum tilt angle for a fixed-tilt array varies significantly throughout the year, ranging from a minimum of 3° in June to a maximum of 69° in December and January, with an annual average of 39°. Correspondingly, incident solar radiation peaks in June at approximately 5.14 kWh/m², while December receives only 49.2% of this peak value, representing the annual minimum. Crucially, to align PV output with the GHP's peak thermal load during the heating season, an alternative winter-optimized tilt of 67° is recommended. This configuration captures an average maximum of 3.14 kWh/m²/day of solar irradiance during the coldest months, thereby directly supporting the system's highest energy demand period. Furthermore, the site experiences a substantial variation in available solar energy hours, with monthly average daily daylight hours ranging from a low of 8.2 hours (in December) to a high of 15.8 hours (in June). In this study, the analysis determined an annual optimum tilt angle of 39° for a fixed-tilt PV system at TBRHSC, which aligns with the established global range of 31° to 45° for comparable mid-latitude locations. This configuration yields an estimated annual average solar irradiance of 3.94 kWh/m²/day. The close agreement of this solar energy yield with the international benchmark of 4.23 kWh/m²/day—representing a deviation of less than 7%—validates the methodological approach and confirms the regional applicability of the findings. The validation of the derived annual optimum tilt angle of 39° against established global data confirms the methodological robustness of the analysis. More significantly, the study's primary applied contribution is the proposal of a load-specific, winter-optimized tilt of 67°—a strategic adaptation designed to enhance the technical and economic feasibility of integrated photovoltaic-geothermal systems operating under the harsh climatic constraints of Northwestern Ontario, Canada. Future work should focus on (1)

extending the work to include the effects of the ambient temperature and the use of anisotropic models (e.g., Hay–Davies sky diffuse model) on the performance of the PV system, (2) a comprehensive economic analysis of large-scale PV-GHP hybrid system integration, and (3) experimental validation of the model's predictions through a field-deployed prototype.

Conflict of Interest

The authors declare no conflict of interest.

Funding

This project was partially funded by Goldcorp Canada Limited – Musselwhite Gold Mine (geothermal heat pump project 2007–2009) and other SWB funding sources (2013–2014) related to the experimental HOBO micro weather-logging station and other systems, which were used to perform experimental measurements to obtain site-specific solar insolation data, essential inputs in the prediction model.

Acknowledgments

The authors would like to thank Ryan Sears and Darin Pretto at TBRHSC for their invitation to Dr. Basel I. Ismail (main author) to visit and tour the TBRHSC facility, facilitating discussions for potential future research collaboration and exploration of applying a hybrid solar-geothermal heat pump system for heating the TBRHSC facility in the extremely cold climate of Northwestern Ontario.

References

[1] Statistics Canada. Focus on Geography Series, 2021 Census of Population. Ottawa (ON): Statistics Canada; 2021 ([cited 2025 Nov 27). Available from: https://www12.statcan.gc.ca/census-recensement/2021/as-sa/fogs-spg/Page.cfm?lang=e&topic=1&dguid=2021A00053558004

[2] Environment and Climate Change Canada. Canadian climate normals. Government of Canada; 2025 (cited 2025 Nov 25). Available from: https://climate.weather.gc.ca/climate_normals/index_e.html

[3] National Renewable Energy Laboratory (NREL). PVWatts calculator. Golden (CO): NREL; 2025 (cited 2025 Nov 25). Available from: https://pvwatts.nrel.gov/pvwatts.php

[4] Thunder Bay Regional Health Sciences Centre. Energy conservation and demand management 2024–2029: 5-year plan. Thunder Bay (ON); 2024 (cited 2025 Nov 25). Available from: https://tbrhsc.net/wp-content/uploads/2024/06/Energy-Usage-Conserv-Plan-2024.pdf

[5] Google Maps. Thunder Bay, Ontario. Google; 2025 [cited 2025 Nov 24]. Available from: https://www.google.ca/maps/place/Thunder+Bay,+ON

[6] Duffie JA, Beckman WA. Solar engineering of thermal processes. 2nd ed. Hoboken (NJ): John Wiley & Sons; 1991.

[7] Al-Sulaiman FA, Ismail B. Estimation of monthly average daily and hourly solar radiation impinging on a sloped surface using the isotropic sky model for Dhahran, Saudi Arabia. Renew Energy. 1997; 11(2): 257-62. https://doi.org/10.1016/S0960-1481(96)00125-5

[8] Shu N, Kameda N, Kishida Y, Sonoda H. Experimental and theoretical study on the optimal tilt angle of photovoltaic panels. J Asian Archit Build Eng. 2006; 5(2): 399-405. https://doi.org/10.3130/jaabe.5.399

[9] Hailu G, Fung AS. Optimum tilt angle and orientation of photovoltaic thermal system for application in Greater Toronto. Sustainability. 2019; 11(22): 6443. https://doi.org/10.3390/su11226443

[10] Abikoye OE, Ogumekan T, Olaboye YO. Determination of optimum tilt angle of photovoltaic solar module for each month of the year: a case study of Offa, Kwara State, Nigeria. Int J Eng Res Technol. 2015; 4(9): 246-53.

[11] Jacobson MZ, Jadhav V. World estimates of PV optimal tilt angles and ratios of sunlight incident upon tilted and tracked PV panels relative to horizontal panels. Sol Energy. 2018; 169: 55-66. https://doi.org/10.1016/j.solener.2018.04.030

[12] Ismail BI, Bujold J. 10 kW solar photovoltaic grid-connected system installed in Fort Frances, Northern Ontario, Canada. In: Proc Int Conf Innovative Technologies; 2015; Dubrovnik, Croatia.

[13] Khan FT, Rashid MN, Alif KMO, Huda ASN. A data-driven approach for comparative estimation of solar PV output in Dhaka using various tilt angle optimization techniques. In: Proc 27th Int Conf Dev Renew Energy Technol (ICDRET); 2024 Jan 11-13; Dhaka, Bangladesh. IEEE. https://doi.org/10.1109/ICDRET60388.2024.10503759

[14] Heibati SM, Marefn W, Saber HH. Developing a model for predicting optimum tilt angle of a PV solar system at different geometric, physical and dynamic parameters. Adv Build Energy Res. 2021; 15(2): 179-98. https://doi.org/10.1080/17512549.2019.1684366

[15] Nazmul RB. Calculating optimum angle for solar panels of Dhaka, Bangladesh for capturing maximum irradiation. In: Proc IEEE Int WIE Conf Electr Comput Eng (WIECON-ECE); 2017 Dec 18-19; Dehradun, India. IEEE. https://doi.org/10.1109/WIECON-ECE.2017.8468880

[16] Manzoor HU, Aaqib SM, Manzoor T, Azeem F, Ashraf MW, Manzoor S. Effect of optimized tilt angle of PV modules on solar irradiance for residential and commercial buildings in different cities of Pakistan: simulation-based studies. Energy Sci Eng. 2025; 13: 1831-45. https://doi.org/10.1002/ese3.70004

[17] Issaq SZ, Talal SK, Azooz AA. Empirical modeling of optimum tilt angle for flat solar collectors and PV panels. Environ Sci Pollut Res Int. 2023; 30: 81250-66. https://doi.org/10.1007/s11356-023-28142-3

[18] Alqaed S, Mustafa J, Almehmadi FA, Jamil B. Estimation of ideal tilt angle for solar-PV panel surfaces facing south: a case study for Najran city, Saudi Arabia. J Therm Anal Calorim. 2023; 148: 8641-54. https://doi.org/10.1007/s10973-022-11812-8

[19] Teyabeen AA, Mohamed F. Estimation of the optimum tilt angle of solar PV panels to maximize incident solar radiation in Libya. Energies. 2024; 17: 5891. https://doi.org/10.3390/en17235891

[20] Haider N, Milcarek RJ, Miller CA, Stechel EB. Impact of panel tilt angle and tracking configuration on solar PV and energy storage capacity for carbon-neutral grid in Arizona. Energies. 2025; 18: 4974. https://doi.org/10.3390/en18184974

[21] Melhem R, Shaker Y, Mazen Ali Mazen F, Abou-Elnour A. Investigation of the optimum solar insolation for PV systems considering the effect of tilt angle and ambient temperature. Energies. 2025; 18: 5257. https://doi.org/10.3390/en18195257

[22] Lu N, Qin J. Optimization of tilt angle for PV in China with long-term hourly surface solar radiation. Renew Energy. 2024; 229: 120741. https://doi.org/10.1016/j.renene.2024.120741

[23] Mansour RB, Khan MAM, Alsulaiman FA, Mansour RB. Optimizing the solar PV tilt angle to maximize the power output: a case study for Saudi Arabia. IEEE Access. 2021; 9: 3052933. https://doi.org/10.1109/ACCESS.2021.3052933

[24] Khan TMY, Elahi M, Soudagar MSM, Kanchan M, Afzal A, Banapurmath NR, et al. Optimum location and influence of tilt angle on performance of solar PV panels. J Therm Anal Calorim. 2020; 141: 511-32. https://doi.org/10.1007/s10973-019-09089-5

[25] Ahmed HM, Calucag LS, Alqahtani H, Noaman NM, Ismail ZM, Alhawi OA. Seasonal analysis of PV performance: optimizing fixed panel angles for maximum efficiency. In: Proc IEEE 9th Int Conf Eng Technol Appl Sci (ICETAS); 2024 Dec 18-20; Istanbul, Turkey. IEEE. https://doi.org/10.1109/ICETAS62372.2024.11120030

[26] Kyranaki N, Kaaya I, Hameed MA, Morlier A, Daenen M. The influence of incidence angle on the reliability of photovoltaic modules: lessons learned. Sol RRL. 2025; 9: 202500477. https://doi.org/10.1002/solr.202500477

[27] Balal A, Dallas T. The influence of tilt angle on output for a residential 4 kW solar PV system. In: Proc IEEE 4th Int Conf Power Energy Appl (ICPEA); 2021 Oct 22-25; Virtual conference. IEEE. https://doi.org/10.1109/ICPEA52760.2021.9639262

[28] Calabrò E. An algorithm to determine the optimum tilt angle of a solar panel from global horizontal solar radiation. J Renew Energy. 2013; 2013: 307547.https://doi.org/10.1155/2013/307547

[29] Bakirci K. General models for optimum tilt angles of solar panels: Turkey case study. Renew Sustain Energy Rev. 2012; 16: 6149-59. https://doi.org/10.1016/j.rser.2012.07.009

[30] Benghanem M. Optimization of tilt angle for solar panel: case study for Madinah, Saudi Arabia. Appl Energy. 2011; 88: 1427-33. https://doi.org/10.1016/j.apenergy.2010.10.001

[31] Elhab BR, Sopian K, Mat S, Lim CH, Sulaiman MY, Ruslan MH, et al. Optimizing tilt angles and orientations of solar panels for Kuala Lumpur, Malaysia. Sci Res Essays. 2012; 7(42): 3758-65.

[32] Siraki AG, Pillay P. Study of optimum tilt angles for solar panels in different latitudes for urban applications. Sol Energy. 2012; 86: 1920-28. https://doi.org/10.1016/j.solener.2012.02.030

[33] Memme S, Fossa M, Rousse D. Best tilt of PV system in Canada: effect of the sky radiation model and climate conditions. Renew Energy. 2025; 254: 123716. https://doi.org/10.1016/j.renene.2025.123716

[34] Rowlands IH, Kemery BP, Beausoleil-Morrison I. Optimal solar-PV tilt and azimuth: an Ontario (Canada) case study. Energy Policy. 2011; 39: 1397-409. https://doi.org/10.1016/j.enpol.2010.12.012

[35] Krishna Y, Karinka S, Fauzan MF, Manihalla PP. An experimental and mathematical investigation of optimal tilt angle and effects of reflectors on PV energy production. MATEC Web Conf. 2021; 335: 03020. https://doi.org/10.1051/matecconf/202133503020

[36] Kaldellis J, Kavadias K, Zafirakis D. Experimental validation of the optimum photovoltaic panels' tilt angle for remote consumers. Renew Energy. 2012; 46: 179-91. https://doi.org/10.1016/j.renene.2012.03.020

[37] Tamoor M, Bhatti AR, Farhan M, Rasool A, Sherefa A. Optimizing tilt angle of PV modules for different locations using isotropic and anisotropic models to maximize power output. Sci Rep. 2024; 14: 30197. https://doi.org/10.1038/s41598-024-81826-9

[38] Al Shammari SA, Karamallah AA, Aljabair S. Optimization of tilt angle and experimental study of standalone PV system for clean energy home supply in Baghdad. FME Trans. 2021; 49: 664-72. https://doi.org/10.5937/fme2103664A

[39] Liu BYH, Jordan RC. Daily insolation on surfaces tilted toward the equator. ASHRAE J. 1962; 3(10): 53.

[40] Klein SA. Calculation of monthly average insolation on tilted surfaces. Sol Energy. 1977; 19: 325. https://doi.org/10.1016/0038-092X(77)90001-9

[41] Pennsylvania State University. Solar radiation on tilted surfaces. University Park (PA): Penn State; (cited 2025 Nov 20). Available from: https://www.e-education.psu.edu/eme810/node/576